

Synaptic Organization of Connections between the Temporal Cortex and Pulvinar Nucleus of the Tree Shrew

Ranida D. Chomsung¹, Haiyang Wei¹, Jonathan D. Day-Brown¹, Heywood M. Petry² and Martha E. Bickford¹

¹Departments of Anatomical Sciences and Neurobiology and ²Psychological and Brain Sciences, University of Louisville, Louisville, KY 40292, USA

Ranida D. Chomsung and Haiyang Wei contributed equally to this work.

We examined the synaptic organization of reciprocal connections between the temporal cortex and the dorsal (Pd) and central (Pc) subdivisions of the tree shrew pulvinar nucleus, regions innervated by the medial and lateral superior colliculus, respectively. Both Pd and Pc subdivisions project topographically to 2 separate regions of the temporal cortex; small injections of anterograde tracers placed in either Pd or Pc labeled 2 foci of terminals in the temporal cortex. Pulvinocortical pathways innervated layers I-IV, with beaded axons oriented perpendicular to the cortical surface, where they synapsed with spines that did not contain gamma amino butyric acid (GABA), likely located on the apical dendrites of pyramidal cells. Projections from the temporal cortex to the Pd and Pc originate from layer VI cells, and form small terminals that contact small caliber non-GABAergic dendrites. These results suggest that cortical terminals are located distal to tectopulvinar terminals on the dendritic arbors of Pd and Pc projection cells, which subsequently contact pyramidal cells in the temporal cortex. This circuitry could provide a mechanism for the pulvinar nucleus to activate subcortical visuomotor circuits and modulate the activity of other visual cortical areas. The potential relation to primate tecto-pulvinocortical pathways is discussed.

Keywords: GABA, pulvinar nucleus, synapse, temporal cortex, *Tupaia belangeri*, ultrastructure

Introduction

In primates and other species with significant visually guided behavior, a large proportion of the dorsal thalamus generates visuosensory- and eye-movement-related signals. Although the visual pathways from the retina through the lateral geniculate nucleus (dLGN) to the striate cortex (V1) have been studied in detail, relatively little is known regarding the synaptic organization of pathways connecting the extrageniculate visual thalamus with the cortex. The purpose of this study was to examine the synaptic organization of thalamocortical terminals and corticothalamic terminals connecting the cortex to well-defined subdivisions of the pulvinar nucleus that receive visual input from the superficial layers of the superior colliculus (SC).

Tree shrews (*Tupaia*) are small, fast moving animals with excellent motion vision and visually guided behavior. Particularly striking features of the tree shrew brain are the greatly enlarged SC, and a correspondingly large pulvinar nucleus. The fact that the tree shrew brain possesses many primate characteristics (Kaas and Preuss 1993; Kaas 2002), led at one time to their classification in the primate order (LeGros Clark 1934; Campbell 1980). Although now classified in the order *Scandentia*, tree shrews still are considered to represent a prototype of early prosimian primates. Therefore, studies of

the connections between the cortex and pulvinar nucleus in the tree shrew should shed light on the organization of these connections in primates.

The tree shrew pulvinar contains 2 tectorecipient subdivisions: the dorsal (Pd) and central (Pc) pulvinar (Lyon et al. 2003a, 2003b). The tectal projections to these 2 subdivisions are organized differently; those to Pd terminate diffusely, whereas those to Pc terminate in a more spatially precise manner (Luppino et al. 1988). In subsequent studies using anterograde and retrograde tracing techniques, as well as electron microscopy, we concluded further that although both Pd and Pc receive topographically organized projections from the SC, the Pd receives additional diffuse projections, which possibly arise from wide-ranging axon collaterals of tectopulvinar cells (Chomsung et al. 2008). We also identified differences in the synaptic arrangements of tectal terminals in the Pd and Pc. These results support the argument that the tectorecipient part of the tree shrew pulvinar nucleus comprises 2 distinct zones.

The aims of the current study were 4-fold. First, we tested whether the Pd and Pc target distinct cortical areas to determine whether these pulvinar subdivisions comprise parallel pathways from the SC to the cortex. Second, we examined the laminar distribution and ultrastructure of pulvinocortical terminals in an effort to determine the cortical cell types targeted by the tectorecipient pulvinar nucleus. Third, we examined the laminar origin and reciprocity of corticopulvinar connections to determine how the organization of the tectorecipient pulvinar nucleus compares to that of other dorsal thalamic nuclei. Finally, we measured the size of corticopulvinar terminals and their postsynaptic targets (to compare to our previous measurements of tectal terminals and their postsynaptic targets, Chomsung et al. 2008) in order to understand how cortical and tectal inputs are distributed on the dendritic arbors of Pd and Pc neurons. Our results define the unique circuitry of the tectorecipient zones of the pulvinar nucleus, and provide the first characterization of the synaptic organization of pulvinocortical projections in any species.

Methods

A total of 27 adult (average weight 175 g) tree shrews (*Tupaia belangeri*); 17 males and 10 females, were used for these experiments. Fourteen tree shrews were used to examine the distribution, morphology and synaptic targets of pulvinocortical terminals labeled by unilateral (10 animals) or bilateral (4 animals) injections of the anterograde tracer biotinylated dextran amine (BDA) in the pulvinar nucleus (6 of these animals were also used for a previous study, Chomsung et al. 2008). Six tree shrews were used to examine the distribution of pulvinocortical cells labeled by injecting the retrograde tracers rhodamine dextran amine (RDA, 3 animals) rhodamine labeled microspheres ("red beads," 1 animal), cholera toxin subunit B (CTB, 1

animal), or fluorogold (FG, 1 animal) in the temporal cortex. Three tree shrews were used to examine the distribution of corticopulvinar cells labeled by injecting the retrograde tracer FG in the pulvinar nucleus. Corticopulvinar cells were also labeled in one animal that received dual injections of BDA and FG in the pulvinar nucleus. Four animals were used to examine the distribution, morphology, and synaptic targets of corticopulvinar terminals labeled by injecting BDA in the cortex. In addition, corticopulvinar terminals were also labeled in one animal that received dual injections of BDA and CTB in the temporal cortex. Selected sections from BDA-injected tree shrews were stained for acetylcholinesterase (AChE) to distinguish the dorsal (Pd) and central (Pc) regions of the pulvinar nucleus (Lyon et al. 2003a). All methods were approved by the University of Louisville Animal Care and Use Committee and conform to the National Institutes of Health guidelines.

Tracer Injections

Tree shrews that received RDA (10K; Molecular Probes, Eugene, OR), BDA (3000 MW; Molecular Probes), FG (Fluorochrome LLC, Denver, CO), CTB (List Biological Laboratories, Inc., Campbell, CA; catalogue #105), or red bead (Lumafleur, Naples FL) injections were initially anesthetized with intramuscular injections of ketamine (100 mg/kg) and xylazine (6.7 mg/kg). Additional supplements of ketamine and xylazine were administered approximately every 45 min to maintain deep anesthesia through completion of the tracer injections. The heart rate was continuously monitored with a MouseOx pulse oximeter (STARR Life Sciences Corp., Pittsburgh, PA). Prior to injection, the tree shrews were placed in a stereotaxic apparatus and prepared for sterile surgery. A small area of the skull overlying the dorsal pulvinar nucleus, central pulvinar nucleus, dorsal temporal cortex, or posterior temporal cortex was removed and the dura reflected.

For all of the pulvinar injections, and 6 of the temporal cortex injections, a glass pipette containing BDA (5% in saline, tip diameter 2 μ m), FG (2% in saline, tip diameter 2–10 μ m), BDA + FG (5% BDA and 2% FG in saline; tip diameter 2 μ m), or BDA + CTB (5% BDA + 1% desalted CTB in 0.1 M phosphate buffer, pH 6.0; tip diameter 2 μ m) was lowered vertically and the tracer was ejected iontophoretically (2 μ A positive current for 15–30 min). For the remaining injections, a 1- μ L Hamilton syringe containing 0.1–0.3 μ L of RDA (10% in saline), or 0.5- μ L red beads (undiluted solution), was lowered vertically into the temporal cortex and the tracers were ejected via pressure. After a 7-day survival period, the tree shrews were given an overdose of sodium pentobarbital (250 mg/kg) and were perfused through the heart with Tyrode solution, followed by a fixative solution of 2% paraformaldehyde and 2% glutaraldehyde (RDA or BDA injections) or 4% paraformaldehyde (BDA, FG, or CTB injections) in 0.1 M phosphate buffer, pH 7.4 (PB).

The brain was removed from the skull, sectioned into 50- μ m-thick slices using a vibratome (Leica VT100E, Leica Microsystems, Bannockburn, IL) and collected in a solution of 0.1 M PB. In some cases, sections were preincubated in 10% methanol in PB with 3% hydrogen peroxide (to react with the endogenous peroxidase activity of red blood cells not removed during the perfusion). The BDA was revealed by incubating sections in a 1:100 dilution of avidin and biotinylated horseradish peroxidase (ABC; Vector Laboratories, Burlingame, CA) in phosphate-buffered saline (0.01 M PB with 0.9% NaCl, pH 7.4) overnight at 4 $^{\circ}$ C. The sections were subsequently rinsed, reacted with nickel-intensified 3,3'-diaminobenzidine (DAB) for 5 min, and washed in PB. RDA and FG were revealed with green or ultraviolet light, or by incubating with a rabbit anti-rhodamine antibody (Chemicon International, Temecula, CA) diluted 1:10 000, or a rabbit anti-FG antibody (Fluorochrome) diluted 1:50 000, followed by a biotinylated goat-anti-rabbit antibody, ABC, and DAB reaction. CTB was revealed using a rabbit-anti-cholera toxin antibody (Sigma, catalogue # C3062) diluted 1:10 000, followed by a biotinylated goat-anti-rabbit antibody (Vector, catalogue # BA-1000), ABC, and DAB reaction. Red beads were revealed under green light illumination. To reveal the distribution of BDA and FG, or BDA and CTB, for confocal microscopy, the BDA was revealed by incubating sections in a 1:100 dilution of streptavidin conjugated to Alexa Fluor 546 (Molecular Probes, Eugene, OR) and the FG or CTB were revealed with the rabbit antibodies listed above followed by a 1:100 dilution of a goat-anti-rabbit antibody conjugated to Alexa Fluor 488 (Molecular Probes). Sections were mounted on slides for light microscopic

examination (BDA, RDA, FG, CTB, and red bead injections) or were prepared for electron microscopy (BDA injections).

AChE Staining

Alternate sections from 13 cases were stained for AChE to distinguish the Pd and Pc (Lyon et al. 2003a). We used a protocol modified from Geneser-Jensen and Blackstad (1971). Briefly, the tissue was rinsed in deionized water, placed in a solution of AChE for 3 h, and then rinsed in saline, followed by deionized water, before reacting with a 1.25% sodium sulfite solution for 1 min. Following deionized water rinses, the tissue was then incubated in a 1% silver nitrate solution for 5 min, rinsed with deionized water and placed in a 5% sodium thiosulfite solution to adjust the contrast of the tissue staining (approximately 5 min). Finally, the tissue was rinsed in saline, and mounted on slides for light microscope examination.

Light Microscopic Data Analysis

A NeuroLucida system and tracing software (MicroBrightField, Inc., Williston, VT) was used to plot the distribution of FG-labeled corticopulvinar cells, BDA-labeled corticopulvinar terminals, RDA-labeled and red bead-labeled pulvinocortical cells, BDA-labeled pulvinocortical terminals, and CTB-labeled corticotectal cells. In some cases, adjacent sections stained for AChE were used to distinguish the borders of the Pd. The NeuroLucida system was also used to create a 3-dimensional (3D) reconstruction of cortical sections and thalamus sections. The distributions of labeled pulvinocortical terminals and pulvinar injection sites were then added to these reconstructions.

Electron Microscopy

Temporal cortex or pulvinar sections that contained BDA-labeled pulvinocortical terminals or corticopulvinar terminals were postfixed in 2% osmium tetroxide, dehydrated in an ethyl alcohol series, and flat embedded in Durcupan resin between 2 sheets of Aclar plastic (Ladd Research, Williston, VT). Durcupan-embedded sections were first examined with a light microscope to select areas for electron microscopic analysis. Selected areas were mounted on blocks, ultrathin sections (70–80 nm, silver-gray interference color) were cut using a diamond knife, and sections were collected on Formvar-coated nickel slot grids. Selected sections were stained for the presence of gamma amino butyric acid (GABA) using previously reported postembedding immunocytochemical techniques (Patel and Bickford 1997; Kelly et al. 2003; Li et al. 2003; Baldauf et al. 2005; Huppé-Gourgues et al. 2006; Chomsung et al. 2008). The GABA antibody (Sigma, catalogue # A2052, used at a dilution of 1:1000–1:2000) and was tagged with a goat-anti-rabbit antibody conjugated to 15-nm gold particles (Amersham, Arlington Heights, IL). The GABA stained sections were air dried and stained with a 10% solution of uranyl acetate in methanol for 30 min before examination with an electron microscope.

Ultrastructural Analysis

Ultrathin sections were examined using an electron microscope. All labeled terminals involved in a synapse were photographed within each examined section. The pre- and postsynaptic profiles were characterized on the basis of size, (shortest width and area measured using a digitizing tablet and Sigma Scan Software; SPSS, Inc., Chicago, IL), the presence or absence of vesicles, and the overlying gold particle density. The ultrastructural features of adjacent terminals were also noted. In the cortex, profiles were considered to be GABAergic if the gold particle density was higher than that found overlying 95% of the BDA-labeled pulvinocortical terminals. In the pulvinar nucleus, profiles were considered to be GABAergic if the gold particle density was higher than that found overlying 95% of the BDA-labeled corticopulvinar terminals.

Computer Generated Figures

Light level photographs were taken using a digitizing camera (Spot RT; Diagnostic Instruments, Inc., Sterling Heights, MI). Confocal images were taken using an Olympus Fluoview laser scanning microscope (BX61W1). Electron microscopic images were taken using a digitizing

camera (SIA-7C; SIA, Duluth, GA) or negatives, which were subsequently scanned and digitized (SprintScan 45i; Polaroid, Waltham, MA). Using Photoshop software (Adobe Systems, Inc., San Jose, CA), the brightness and contrast were adjusted to optimize the images. Plots and 3D reconstructions of cell and terminal distributions were generated using a NeuroLucida system (MicroBrightField, Inc., Williston, VT).

Results

Topography of Pulvinocortical Projections

To determine the distribution of pulvinocortical projections, we injected the pulvinar nucleus with BDA (Fig. 1) to label

terminals by anterograde transport. We placed injections within the Pd and Pc, both of which receive input from the SC. As previously described (Chomsung et al. 2008), these injections resulted in the retrograde labeling of cells in the lower stratum griseum superficiale (SGS) and stratum opticum (SO) of the SC. Injections that invaded the external medullary lamina (LME; Fig. 1*A,B*) also labeled cells in the temporal cortex (Fig. 2*B*), likely due to uptake by corticothalamic and/or corticotectal axons that travel in the LME. The smaller injections, which were confined to the pulvinar nucleus and did not involve the LME, labeled terminals, but not cells, in the temporal cortex (Figs 2*A* and 3). In addition, pulvinar injections

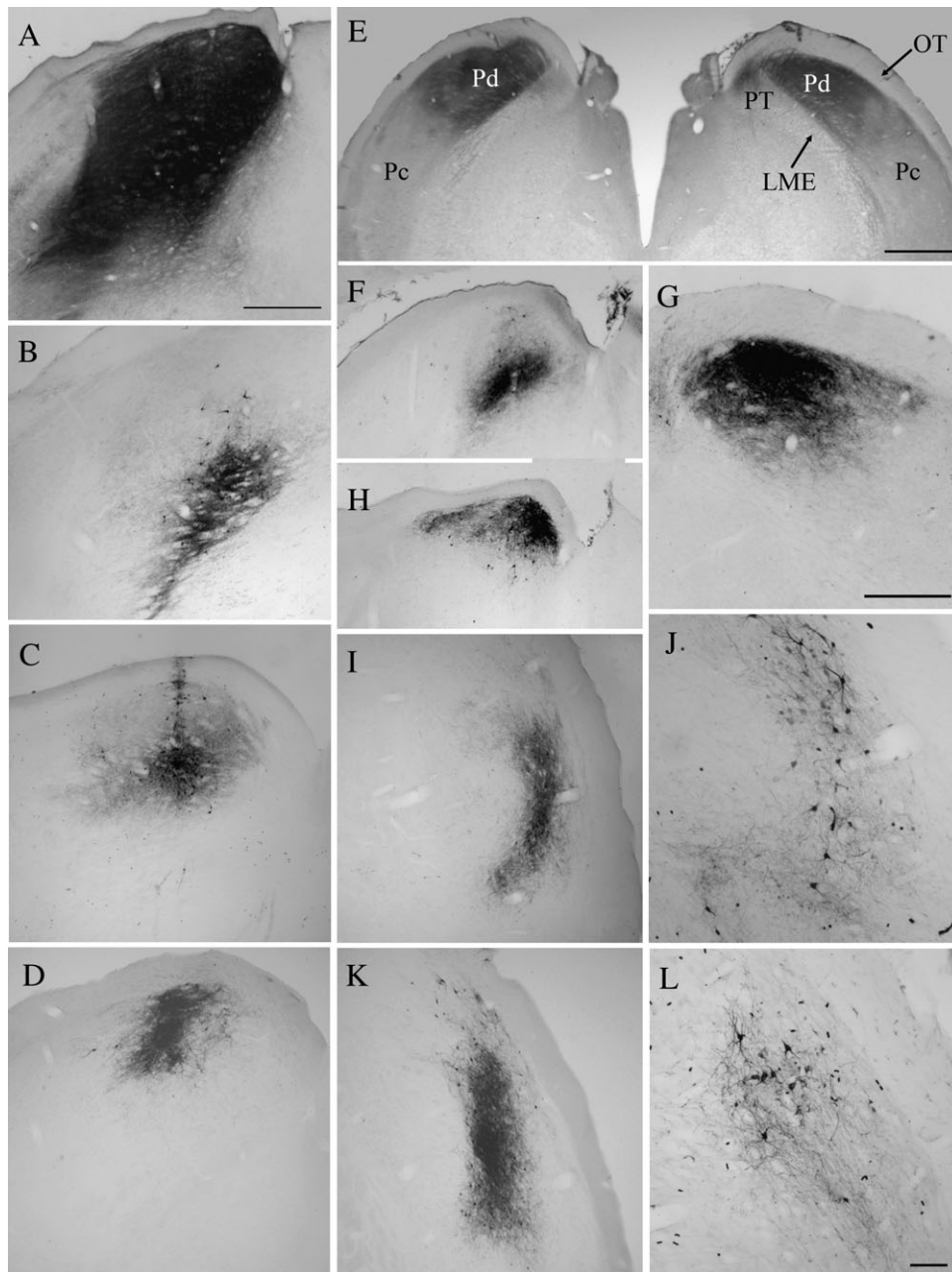


Figure 1. The micrographs illustrate the biotinylated dextran amine injection sites in the pulvinar nucleus that either covered both Pd and Pc subdivisions (*A, B*) or were confined to either the Pd (*C–G*) or the Pc (*I–L*). Most injections were confined to the pulvinar nucleus, but in some cases invaded the underlying external medullary lamina (LME, panels *A* and *B*) or PT (panel *E*, right). Scale bar in *A* = 500 μ m and applies to (*A–D*), (*F*), (*H*), (*I*), and (*K*). Scale bar in (*E*) = 1 mm. Scale bar in (*G*) = 500 μ m. Scale bar in (*L*) = 100 μ m and applies to (*J*).

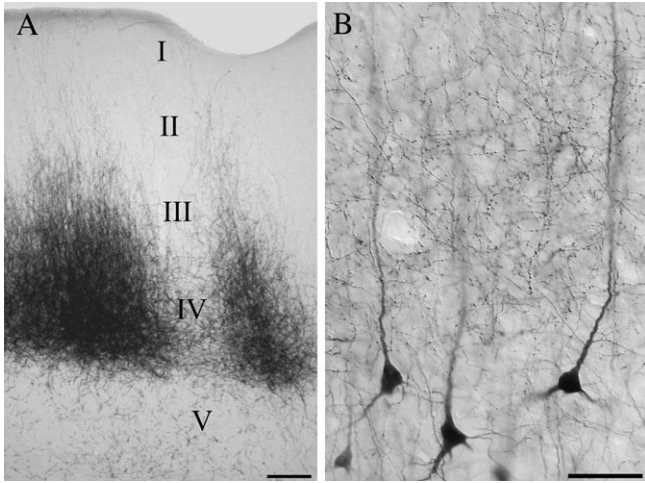


Figure 2. Micrographs illustrate the laminar distribution of pulvinocortical terminals in the temporal cortex. Injections confined to the Pd and/or Pc label terminals that are most densely distributed in layer IV, but extend through layer I (A). Injections that involved the external medullary lamina labeled terminals in layers I–IV, as well as cells in layers V and VI. (B) Shown are pulvinocortical terminals overlapping the apical dendrites of layer V projection cells. Scale in (A) = 100 μ m. Scale in (B) = 50 μ m.

labeled terminals in the caudate nucleus, putamen, and amygdala (data not shown).

Injections restricted to the Pd or Pc labeled terminals in restricted regions of the temporal cortex (Figs 3 and 4). A consistent finding was that small injection sites labeled 2 discrete foci of pulvinocortical terminals. To determine the topography of these projections, we used a NeuroLucida system to reconstruct the patches of labeled terminals in 3 dimensions. As illustrated in Figure 5, the labeled pulvinocortical axons terminated topographically within an area of the posterior temporal cortex, and additionally in an area of the more rostral/dorsal temporal cortex, which we will hereafter refer to as T1 and T2, respectively. As injections in the pulvinar nucleus shifted from rostral to caudal, the patches of labeled terminals shifted from caudal to rostral. Figure 5 also demonstrates that dual topographic projections were labeled by either Pd or Pc injections.

Because each injection site also labeled tectopulvinar cells in restricted regions of the medio-lateral dimension of the SC (described in detail in Chomsung et al. 2008), which has been mapped using physiological recording techniques (Lane et al. 1971), we approximated the representations of the visual field that would presumably be transferred from the SC, through the pulvinar nucleus, to the temporal cortex. These results suggest that the upper visual field is represented in the caudal regions of the temporal cortex, whereas the lower visual field is represented in more rostral regions (summarized in Fig. 12A). Approximation of peripheral or central visual field representations was not possible because the pulvinar injections labeled tectopulvinar cells in bands that spanned the rostro-caudal dimension of the SC (Fig. 9A; Chomsung et al. 2008).

The distribution of pulvinocortical cells labeled following retrograde tracer injections into the temporal cortex confirmed the general topography of pulvinocortical projections. Injections in caudal regions of the temporal cortex labeled cells in more rostral/dorsal regions of the pulvinar nucleus (Fig. 6C,D), whereas injections in the rostral temporal cortex labeled cells in the caudal/ventral pulvinar nucleus (Fig. 6E,F).

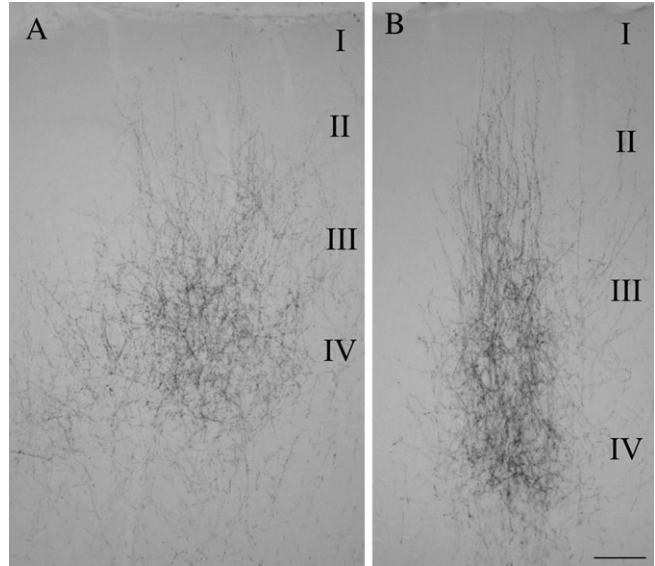


Figure 3. Micrographs illustrate the distribution of pulvinocortical terminals in 2 cortical areas of the temporal cortex resulting from a single injection of biotinylated dextran amine in the pulvinar nucleus. (A and B) Illustrate patches of terminals labeled in area T1 and T2, respectively (locations of these areas are shown in Fig. 5). The approximate laminar boundaries are indicated. Scale = 100 μ m.

Laminar Distribution and Synaptic Targets of Pulvinocortical Terminals

The terminals labeled following both large and small pulvinar injections were most densely distributed in layer IV, but extended through layers III and II to layer I (Figs 2A, 3). Compared with the striate cortex, cortical layers are difficult to discern in the temporal cortex. However, the retrograde labeling of layer V cells following a large pulvinar injection (which invaded the LME, Fig. 1A) served to confirm that the majority of pulvinocortical terminals were distributed above layer V (Fig. 2B). The laminar distribution and morphology of terminals was similar in T1 and T2. However, terminals in T1 tended to be more densely distributed in layer IV than in more superficial layers (Fig. 3A), whereas pulvinocortical terminals in T2 tended to be more evenly distributed through layers IV–I (Fig. 3B), forming discrete columns of terminals. This slight difference in the laminar distribution of pulvinocortical terminals was accentuated in the most rostral regions of the T2, where the cortex is thicker than that of the T1 projection zone.

In both the T1 and T2, the pulvinocortical axons gave rise to boutons which were distributed along the axon in a “beads on a string” pattern (Fig. 2B). The axons were generally oriented perpendicular to the cortical surface, and single axons could be followed from layer IV to layer I. We examined the synaptic targets of a total of 387 labeled pulvinocortical terminals within the 2 projection zones of 4 tree shrews. All blocks analyzed at the ultrastructural level contained terminals in lamina I–IV. The labeled terminals made a total of 442 synaptic contacts (226 synapses in T1 and 216 synapses in T2). Examples of synaptic contacts in the 2 projection zones are illustrated in Figure 7. Similar synaptic contacts were observed in all cases.

The size of pulvinocortical terminals was similar in T1 and T2 (shortest width $0.62 \pm 0.15 \mu$ m in T1 and $0.68 \pm 0.16 \mu$ m in T2). In both areas we found that pulvinocortical terminals form asymmetric contacts with spines and small dendrites (shortest width $0.40 \pm 0.13 \mu$ m in T1 and $0.44 \pm 0.12 \mu$ m in T2). Most

pulvinocortical terminals formed single synapses (53.54% in T1 and 48.68% in T2; Fig. 7D,F), whereas other contacts could be classified as perforated (32.82% in T1 and 37.03% in T2; Fig. 7A, B, E, and H). Pulvinocortical terminals were also observed to

form multiple synapses (13.64% in T1 and 14.29% in T2; Fig. 7C,G).

Each examined section was also stained for GABA using postembedding immunocytochemical techniques to determine whether pulvinocortical terminals contact GABAergic or non-GABAergic cells. With the assumption that pulvinocortical terminals are non-GABAergic, the gold particle density overlying the labeled terminals was used as a measure of background staining, which is fixation dependent and varies from case to case (T1 animal 1 mean density = 14.06 ± 11.59 gold particles/ μm^2 , $n = 103$; T1 animal 2 mean density = 4.44 ± 4.38 gold particles/ μm^2 , $n = 95$; T2 animal 1 mean density = 10.69 ± 7.98 gold particles/ μm^2 , $n = 100$; T2 animal 3 mean density = 14.34 ± 10.44 gold particles/ μm^2 , $n = 89$). Using this criteria, all postsynaptic targets of pulvinocortical terminals were found to be non-GABAergic (T1 animal 1 mean density = 8.79 ± 9.02 , $n = 119$; T1 animal 2 mean density = 5.64 ± 7.49 , $n = 107$; T2 animal 1 mean density = 5.02 ± 6.08 , $n = 119$; T2 animal 3 mean density = 8.44 ± 7.12 , $n = 97$).

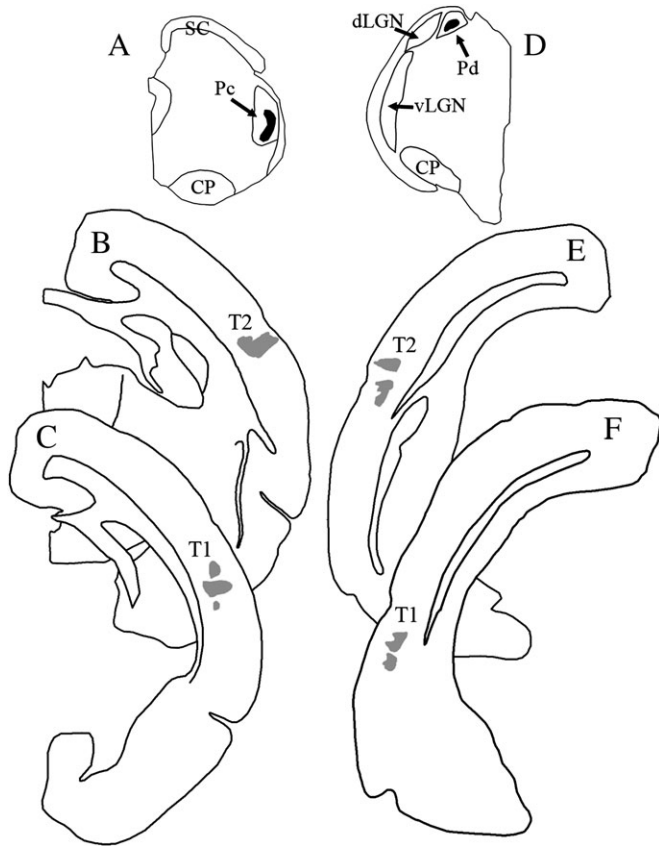


Figure 4. Lontophoretic injections of biotinylated dextran amine in the pulvinar nucleus label 2 foci of terminals in the temporal cortex. Injection sites in the caudal Pc (A) and rostral Pd (D) are shown in black, and the resulting dual terminal distributions (T1 and T2) are shown in gray (B, C, E, F).

Laminar Origin and Reciprocity of Corticopulvinar Connections

Injections of FG that were confined to the Pd and/or Pc (and did not involve the LME) labeled cells exclusively in layer VI of the temporal cortex (Figs 6A, B, and 9A). Small injections labeled 2 clusters of cells in T1 and T2 (Fig. 8), whereas larger injections labeled a continuous band of cells in the temporal cortex (Fig. 9D,E).

Injections of FG that included, but were not confined to the pulvinar nucleus, labeled cells in both layers V and VI of the cortex. These results suggest that all corticothalamic projections to the Pd and Pc originate from layer VI of the temporal cortex, whereas projections to adjacent nuclei (ventral pulvinar and lateral intermediate nucleus) may originate from cells in both layers V and VI (although the involvement of the LME complicates interpretation).

To test whether corticopulvinar and pulvinocortical connections are reciprocal, we injected both BDA and FG from the same pipette into a single site in the pulvinar nucleus (Fig. 9C).

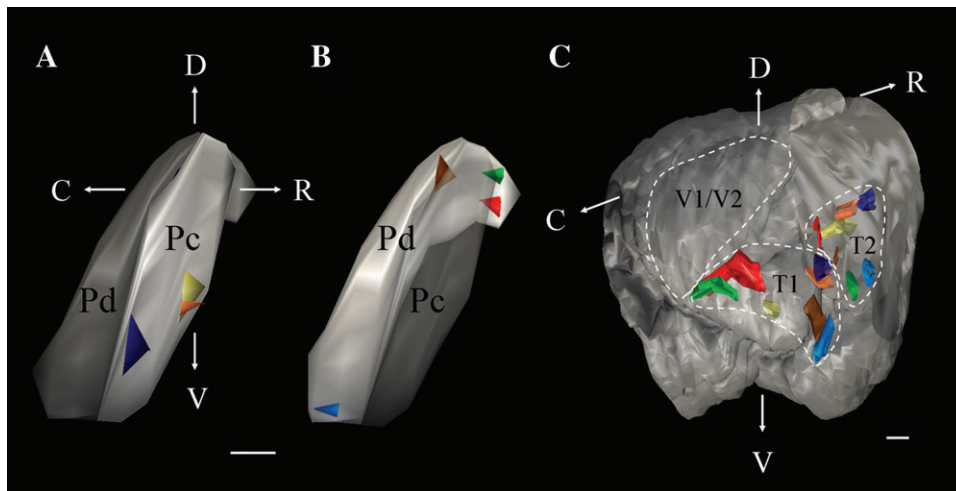


Figure 5. Single injections of biotinylated dextran amine in the pulvinar nucleus label 2 terminal foci in the temporal cortex (T1 and T2). Three-dimensional reconstructions (lateral views) illustrate the location of injections in the Pc (A) and Pd (B) and the resulting distribution of pulvinocortical terminals (C). Each color indicates a single injection site in the pulvinar nucleus and the resulting 2 foci of pulvinocortical terminals. C, caudal, D, dorsal, R, rostral, V, ventral, V1/V2, primary and secondary visual cortex. Scale for (A) and (B) = 0.5 mm, scale for (C) = 1 mm.

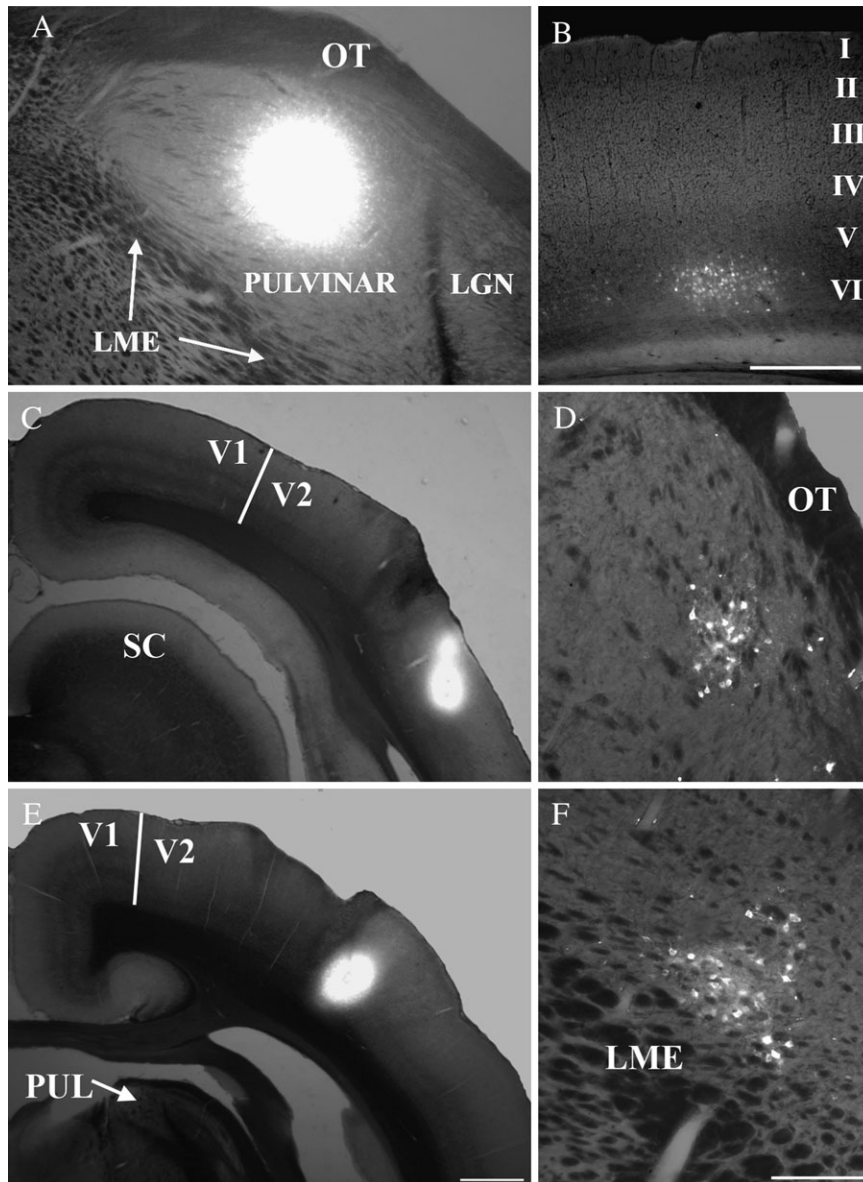


Figure 6. Corticopulvinar and pulvinocortical projections are topographically organized. A fluorogold injection that included both the Pd and Pc (A) labeled cells in layer VI of restricted regions of the temporal cortex (B). A fluorogold injection in the posterior temporal cortex (T1, C) labeled cells in the dorsal/rostral Pc (D), whereas a fluorogold injection in the more rostral/dorsal temporal cortex (T2, E) labeled cells in the caudal/ventral Pc (F). Scale bar in (B) = 500 μ m and applies to (A), scale bar in (E) = 1 mm and applies to (C). Scale bar in (F) = 250 μ m and applies to (D). LGN, lateral geniculate nucleus, LME, external medullary lamina., OT, optic tract, PUL, pulvinar nucleus, V1, striate cortex, V2, secondary visual cortex.

This resulted in closely overlapping distributions of cells and terminals in the temporal cortex (Fig. 9A,D,E). Similarly, when we injected both BDA and CTB from the same pipette into the temporal cortex (Fig. 9F), we found that pulvinocortical cells and corticopulvinar terminals overlapped extensively within the pulvinar nucleus (Fig. 9B,G,H).

Morphology and Synaptic Targets of Corticopulvinar Terminals

Figure 10A illustrates the morphology of terminals in the Pc labeled by anterograde transport from an injection in T2. The labeled axons were of small caliber and gave rise to small diffusely distributed boutons that emanate from short stalks. For comparison, Figure 10B illustrates the morphology of axons

in the pretectum (PT) labeled from the same injection site. These corticopretectal axons (which are shown at the same magnification as the corticopulvinar axons in Fig. 10A), are thicker and give rise to larger boutons. All terminals in the Pd and Pc labeled following BDA injections in either T1 or T2 exhibited a morphology that was similar to that illustrated in Figure 10A.

We examined the synaptic targets of a total of 417 labeled corticothalamic terminals in the pulvinar nucleus of 3 tree shrews. Each labeled terminal made a single synaptic contact in the sections examined. Examples of synaptic contacts are illustrated in Figure 11.

In both Pd and Pc, we found that terminals labeled from the temporal cortex were small profiles that contained round vesicles (RS profiles; mean terminal width in Pd = $0.46 \pm$

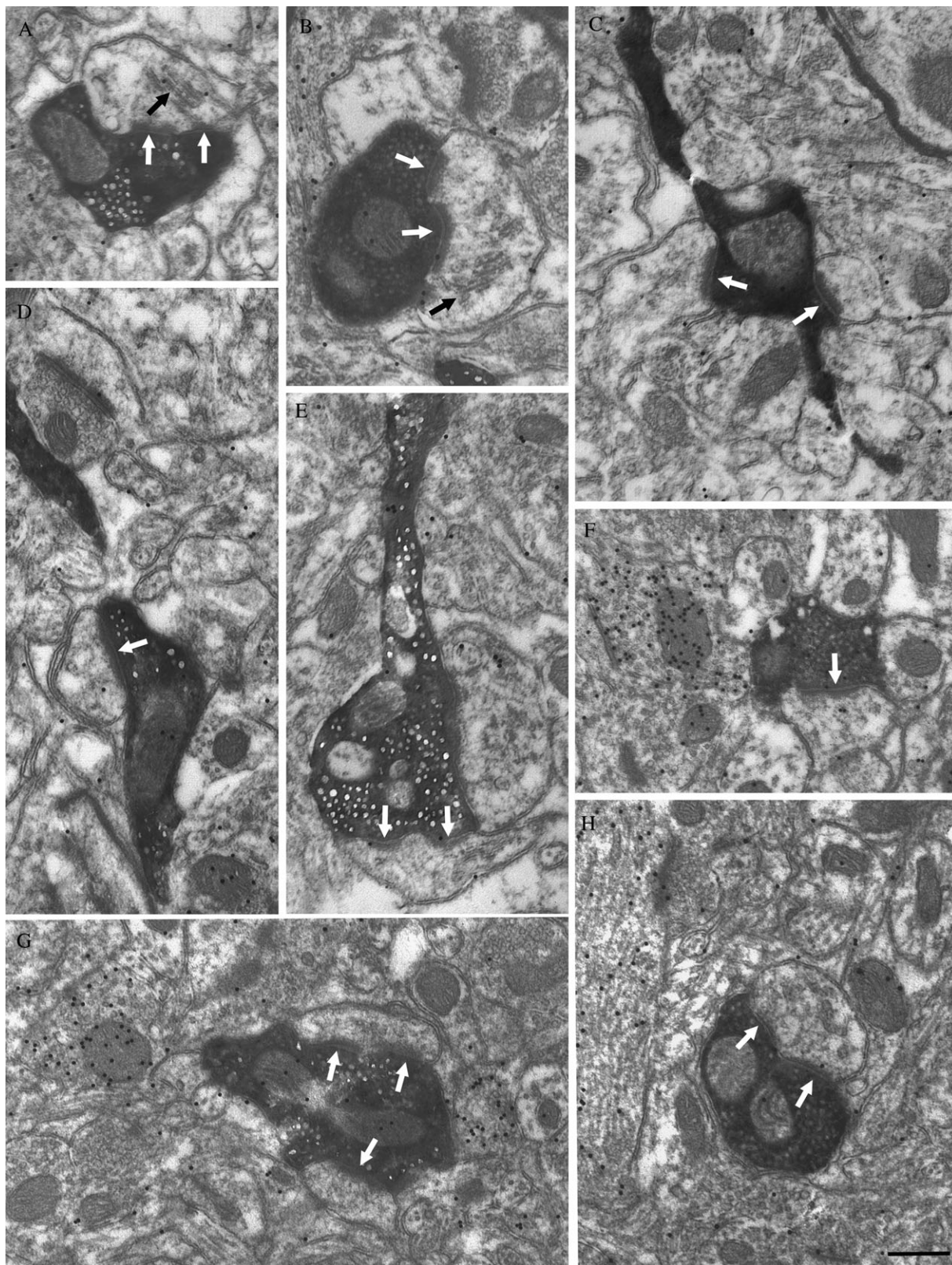


Figure 7. Most pulvinocortical terminals contact (white arrows) non-GABAergic (low density of overlying gold particles) spines (identified by size and occasionally the presence of a spine apparatus, black arrows) with asymmetric synapses. The ultrastructure of pulvinocortical terminals in the T2 (A, B, and C) and T1 (D-H) is illustrated. Single (D, F) and perforated (A, B, E, H) synapses were identified, and some terminals contacted multiple profiles (C, G). Scale bar = 0.5 μ m and applies to all panels.

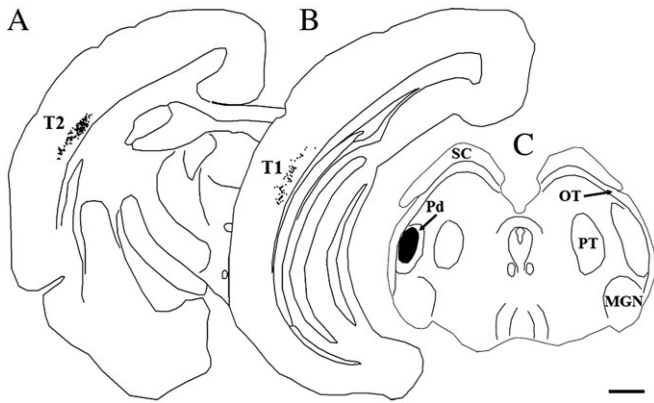


Figure 8. Corticopulvinar cells (black dots) are labeled in layer VI of 2 zones T2 (A) and T1 (B) following single injections of fluorogold in the pulvinar nucleus (C), shown in black). Scale bar = 1 mm.

0.10 μm ; mean terminal width in Pc = $0.48 \pm 0.13 \mu\text{m}$) that contacted relatively small caliber dendrites (shortest widths of postsynaptic dendrites: $0.73 \pm 0.29 \mu\text{m}$ in Pd and $0.79 \pm 0.33 \mu\text{m}$ in Pc) with thick postsynaptic densities. There was no significant difference in the sizes of corticopulvinar terminals or their postsynaptic dendrites in the Pd and Pc (Student's *t*-test). However, the sizes of corticopulvinar terminals and their postsynaptic dendrites were both found to be significantly smaller (Student's *t*-test, $P < 0.001$) than our previous measurements (Chomsung et al. 2008) of tectopulvinar terminals (Pd, 0.62 ± 0.22 ; Pc 0.62 ± 0.21) and their postsynaptic dendrites (Pd, 1.07 ± 0.67 , Pc, 0.97 ± 0.46).

Each examined section was also stained for GABA using postembedding immunocytochemical techniques to determine whether pulvinocortical terminals contact GABAergic interneurons or non-GABAergic projection cells. With the assumption that corticopulvinar terminals are non-GABAergic, the gold particle density overlying the labeled terminals was used as a measure of background staining, which is fixation dependent and varies from case to case (Pd animal 1 mean density = 2.58 ± 2.92 gold particles/ μm^2 , $n = 100$; Pc animal 2 mean density = 4.36 ± 5.26 gold particles/ μm^2 , $n = 102$; Pc animal 2 mean density = 7.67 ± 6.0 gold particles/ μm^2 , $n = 101$; Pc animal 3 mean density = 6.68 ± 7.75 gold particles/ μm^2 , $n = 114$). Using this criterion, we found that the majority of dendrites postsynaptic to labeled terminals were non-GABAergic (Pd animal 1 mean density = 2.02 ± 2.22 gold particles/ μm^2 , $n = 89$; Pc animal 2 mean density = 3.23 ± 2.55 gold particles/ μm^2 , $n = 90$; Pc animal 2 mean density = 3.33 ± 2.96 gold particles/ μm^2 , $n = 93$; Pc animal 3 mean density = 3.41 ± 4.19 gold particles/ μm^2 , $n = 108$).

The gold density overlying the remaining profiles was significantly higher (Student's *t*-test $P < 0.001$ in each case) than that overlying the labeled corticopulvinar terminals (Pd animal 1 mean density = 22.03 ± 12.26 gold particles/ μm^2 , $n = 11$; Pc animal 2 mean density = 36.97 ± 16.43 gold particles/ μm^2 , $n = 12$; Pc animal 2 mean density = 34.10 ± 12.84 gold particles/ μm^2 , $n = 8$; Pc animal 3 mean density = 37.82 ± 19.20 gold particles/ μm^2 , $n = 6$). Overall, 11 of 100 or 11% of the postsynaptic profiles in the Pd, and 26 of 317 or 8.2% of the postsynaptic profiles in Pc were GABAergic. Of these GABAergic postsynaptic profiles, 63.6% (7/11)

in Pd and 65.4% or (17/26) in Pc contained vesicles (e.g., Fig. 11A).

Discussion

Figure 12 summarizes the main findings of this study of 859 pulvinocortical and corticopulvinar synapses, and of our previous study of 539 tectopulvinar synapses (Chomsung et al. 2008). We found that the Pd and Pc are reciprocally and topographically connected with 2 regions of the temporal cortex. Projections from the Pd and Pc contact non-GABAergic spines in layers I-IV of the temporal cortex, and projections from cells in layer VI of the temporal cortex primarily contact small caliber non-GABAergic dendrites in the Pd and Pc. Compared with tectopulvinar terminals, corticopulvinar terminals are smaller and contact smaller caliber dendrites in the Pd and Pc. The difference in the size of the dendrites postsynaptic to these 2 terminal types suggests that corticopulvinar terminals are located distal to tectopulvinar terminals on the dendritic arbors of pulvinar projection cells. In the discussion that follows we will relate these results to previous studies of the tree shrew and other species, and consider how the classification of thalamic nuclei into first and higher order applies to the organization of the tectorecipient pulvinar nucleus.

Reciprocal Topographic Pulvinocortical Connections Define 2 Temporal Areas

Our results indicate that the tectorecipient pulvinar nucleus is reciprocally connected with the temporal cortex: layer VI cells in the temporal cortex project to the Pd and Pc, and the Pd and Pc project to layers I-IV of the temporal cortex. Our results also indicate that the projections from the Pd and Pc to the temporal cortex are topographic. Small injections in the pulvinar resulted in discrete patches of labeled terminals in the temporal cortex, and small injections in the temporal cortex labeled discrete groups of cells in the pulvinar nucleus. Both sets of experiments indicate that the caudal pulvinar nucleus is connected with more rostral regions of the temporal cortex, whereas the rostral pulvinar connects to more caudal regions of the temporal cortex. These results corroborate the findings of Luppino et al. (1988), who described the distribution of pulvinar cells labeled by retrograde transport following injections in dorsal (Td) and ventral (Tv) subdivisions of the tree shrew temporal cortex, as well as Diamond et al. (1970) and Harting et al. (1973) who described the distribution of degenerating thalamocortical cells and terminals following cortical or thalamic lesions respectively.

However, although the current and past retrograde tracing studies, and previous anterograde and retrograde degeneration studies suggest that the rostral/dorsal temporal cortex receives input primarily from the Pc, and the posterior/ventral temporal cortex receives input primarily from the Pd, our anterograde tracing studies indicate that the Pc and Pd send dual topographic projections to both areas. We previously found that the Pd receives input from the medial SC (which responds to upper visual field stimuli), whereas the Pc receives input from the lateral SC (which responds to lower visual field stimuli). Thus, we conclude that the Pd and Pc together may respond to the entire visual field (in agreement with Lyon et al. 2003b). With this in mind, our anterograde tracing results suggest that the entire visual field is

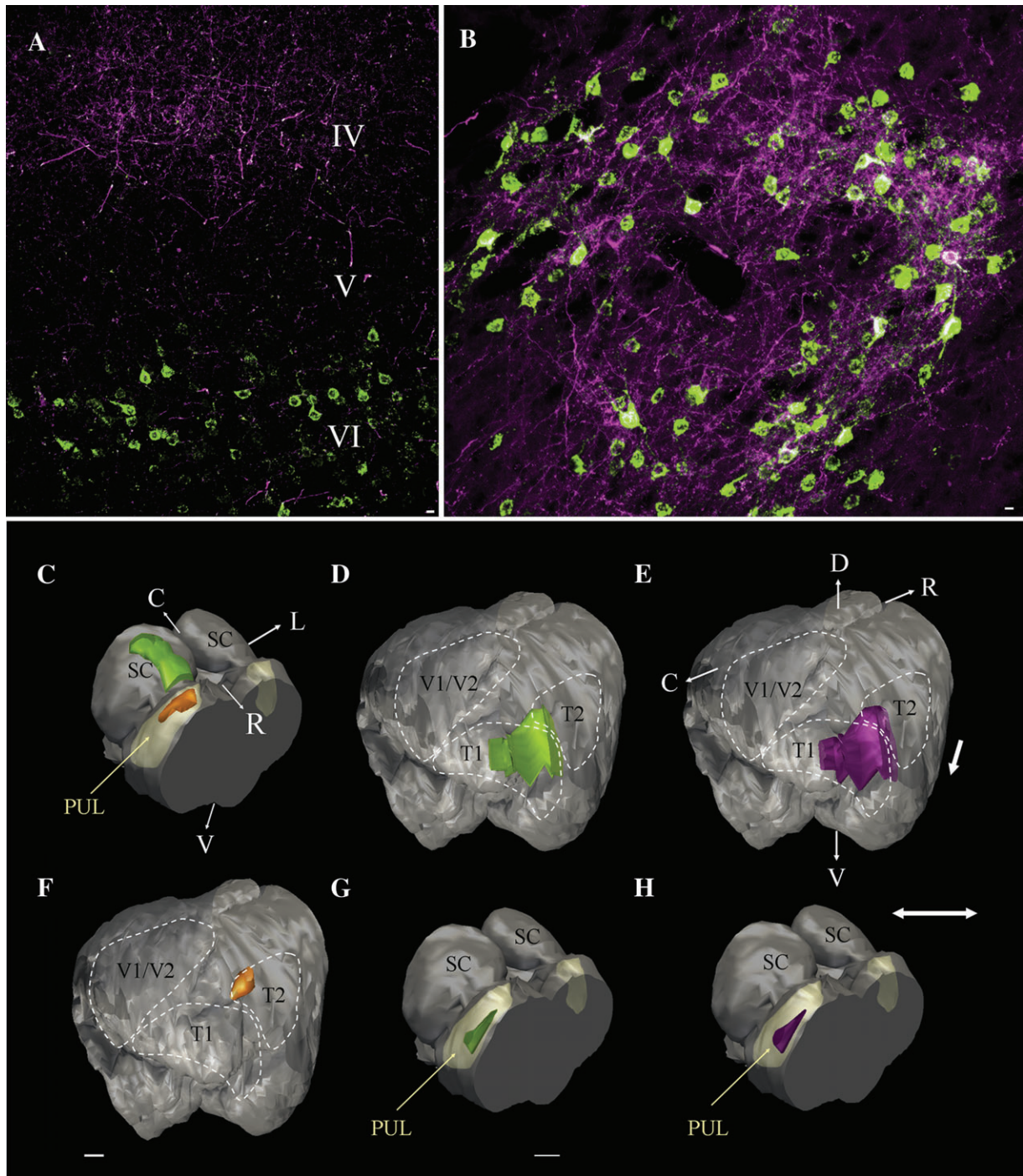


Figure 9. The pulvinar nucleus and temporal cortex are reciprocally connected. (A) The confocal image of the temporal cortex illustrates the overlapping distributions of pulvinocortical terminals (purple, in layer IV) and corticopulvinar cells (green, in layer VI) labeled by a dual injection of biotinylated dextran amine and fluorogold in the tectorecipient pulvinar nucleus (PUL, yellow; injection site is depicted in orange in panel (C), also illustrated in Figure 1E, left pulvinar). (B) The confocal image of the pulvinar nucleus illustrates the overlapping distributions of pulvinocortical cells (green) and corticopulvinar terminals (purple) labeled by a dual injection of biotinylated dextran amine and CTB in the temporal cortex (injection site depicted in orange in panel (F)). Three-dimensional reconstructions of the case illustrated in panel (A) show the overlapping distributions of corticopulvinar cells (D, green) and pulvinocortical terminals (E, purple) which formed a band within T1 and T2. Tectopulvinar cells labeled from the same pulvinar injections site are distributed in a band that is restricted in the medio-lateral dimension (C, green). Three-dimensional reconstructions of the case illustrated in panel (B) show the distributions of pulvinocortical cells (G, green) and corticopulvinar terminals (H, purple) which overlapped within a restricted region of the pulvinar nucleus. C, caudal, D, dorsal, R, rostral, V, ventral, V1/V2, primary and secondary visual cortex. Scale bars in (A) and (B) = 10 μ m. Scale in (G) = 1 mm and applies to (C) and (H). Scale in (F) = 1 mm and applies to (D) and (E).

represented in 2 separate areas of the temporal cortex (summarized in Fig. 12A). This corroborates the original division of the temporal cortex into Td and Tp based on the

pattern of corticocortical cells and terminals labeled following tracer injections in V1 (Sesma et al. 1984). The finding that single injections in V1 labeled patches of cells and terminals in

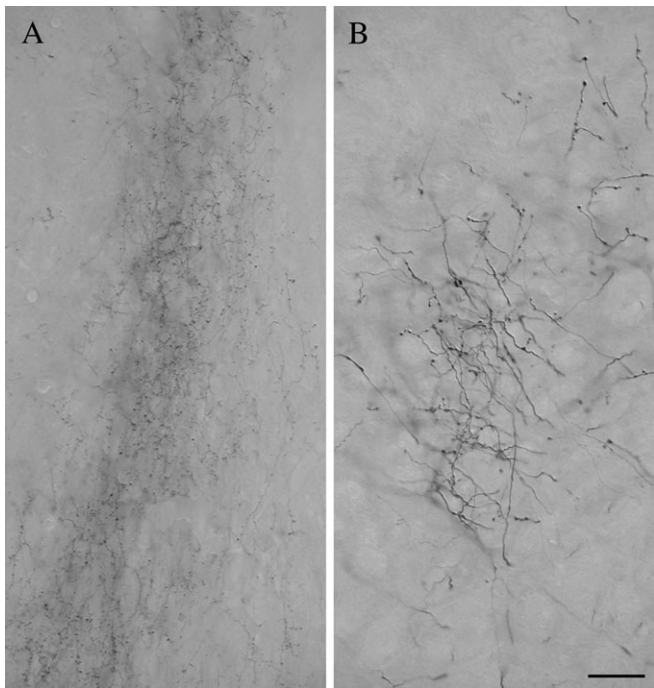


Figure 10. The micrographs illustrate the morphology of axons and terminals labeled by an injection of BDA in the temporal cortex. In the pulvinar nucleus (A), the labeled axons are of fine caliber and give rise to small boutons. In the PT (B), axons labeled from the same cortical injection site are thicker and give rise to larger boutons. Scale bar = 30 μ m and applies to both panels.

2 distinct areas supported the view that each area contained a complete map of the visual field.

More recently, the temporal cortex of the tree shrew has been subdivided into multiple smaller areas based on architectonics (Wong and Kaas 2009). Comparison of the cortical areas defined by pulvinar projection patterns to those defined by cytoarchitectural features indicates that the Pd and Pc project most densely to the posterior and inferior temporal cortex, with some extension into the dorsal temporal and parietal cortex. Thus, although our results support the view that projections from the Pd and Pc define 2 topographically organized cortical areas, further studies of these projections in relation to cytoarchitecture, corticocortical projection patterns, and/or physiological response properties may reveal that the cortical targets of the Pd and Pc constitute multiple functional subdivisions. A particularly important question for future studies is whether activity patterns of Pd and Pc pulvinocortical cells differ as a result of the diffuse tectal projection that terminates only in Pd, and whether diffuse tectopulvinar terminals in the Pd differentially contact cells that project to the temporal cortex, striatum or amygdala.

Finally, single cells in the tree shrew pulvinar nucleus might branch to innervate the 2 cortical targets (as suggested in Fig. 12B), although our results do not rule out the possibility that these projections arise from different cell types located adjacent to one another. Evidence for collateral projections was provided by Diamond and Hall (1969) who noted that large lesions of the tree shrew temporal cortex produced widespread degeneration of pulvinar neurons, but little discernable degeneration was observed following small lesions in the temporal cortex. Harting et al (1973) subsequently searched for the presence of sustaining collateral pulvinocortical projections in

a large series of experiments with precisely placed pulvinar lesions. However, a single focus of degenerating pulvinocortical terminals was always observed in the temporal cortex. The difference in our results may be due to the more sensitive anterograde tracing techniques that are now available. In fact, studies in other species indicate that branching pulvinar axons may be quite common. For example, Rockland et al. (1999) examined the morphology and distribution of cortical projections originating in the primate lateral pulvinar. Reconstructions of individual labeled axons revealed widespread terminations in multiple layers, often with several foci. In addition, cells in the pulvinar nucleus or its homologs have been shown to be double-labeled from dual tracer injections placed in distinct cortical areas (Kaufman et al. 1984; Cusick et al. 1985; Tong and Spear 1986; Miceli et al. 1991).

Pulvinocortical Terminals Contact Spines

This study is the first to examine the ultrastructure of pulvinocortical terminals in any species. We found that terminals in the temporal cortex labeled via tracer injections in the Pd or Pc formed asymmetrical synapses on the spines of non-GABAergic neurons. These contacts are similar to those observed for geniculostriate terminals of the cat, ferret, and monkey (Einstein *et al.* 1987; Ding and Casagrande 1998; Latawiec et al. 2000; Erisir and Dreusicke 2005; Nahmani and Erisir 2005; Anderson et al. 2009). However, most geniculostriate axons form restricted arbors (in the tree shrew, axons originating from laminae 1, 2, 4, and 5 of the dLGN terminate in layer IVa or IVb of the striate cortex), overlapping the horizontally oriented dendritic fields of spiny stellate cells (Raczkowski and Fitzpatrick 1990; Muly and Fitzpatrick 1992). In the cat, spiny stellate cells were found to be prominent in layer IV of the striate cortex, but were not found in the temporal (auditory) cortex (Smith and Populin 2001). It is not yet known whether the temporal cortex of the tree shrew contains spiny stellate cells but, in any case, the more widespread distribution of pulvinocortical axons, oriented perpendicular to the cortical surface from layer IV through layer I, suggests that spines on the apical dendrites of pyramidal cells might be a more likely target of pulvinocortical terminals.

Pulvinocortical projections could terminate on spines on the apical dendrites of layer V projection cells. In this case, projections from the pulvinar nucleus to the temporal cortex might activate subcortical visuomotor circuits via contacts on corticotectal cells, corticopretectal cells and/or cortico-striate cells. Pulvinocortical terminals might also contact spines on the apical dendrites of corticocortical pyramidal cells. Extensive projections from the temporal cortex to the striate cortex have been identified in the tree shrew (Sesma et al. 1984; Lyon et al. 2003b), so it is possible that pulvinocortical projections to the temporal cortex could additionally contribute to the contextual modulation of striate activity patterns by regulating the activity of corticocortical cells. In either case, the density of projections from the Pd and Pc to the temporal cortex suggests that tectopulvinar pathways can significantly impact cortical activity patterns.

Synaptic Organization of the Pd and Pc: “Second Order” Nuclei

The dLGN is considered a “first order” thalamic nucleus because the activity of geniculocortical neurons is driven by

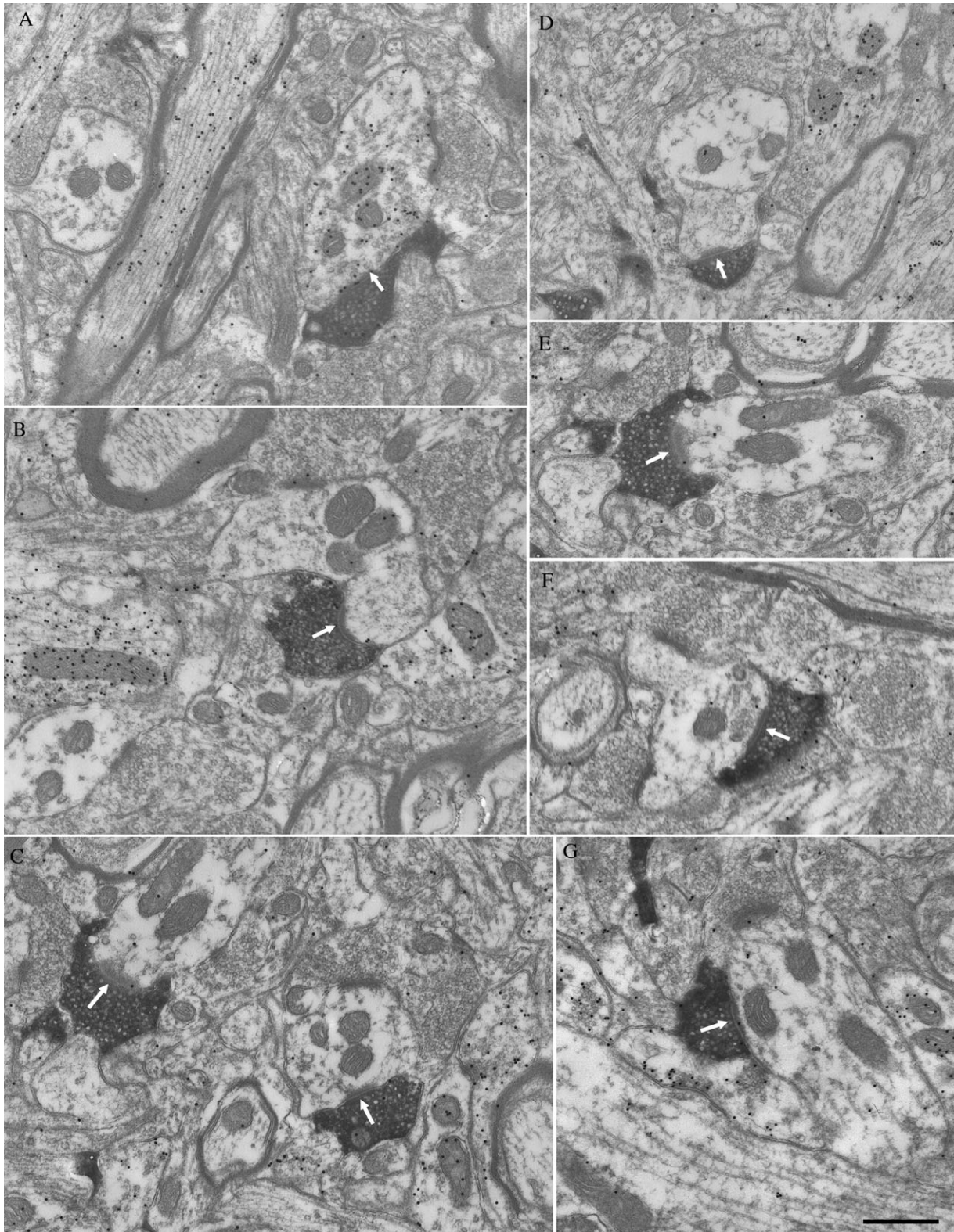


Figure 11. Examples of the corticothalamic terminals in Pc labeled by the anterograde transport of BDA from T2. All terminals are small profiles and primarily contact (white arrows) GABA-negative (low density of the gold particles) profiles (B-G). A few contacts are made with GABA-positive (high density of the gold particles) profiles that contain synaptic vesicles (A). Scale bar = 0.5 μ m.

large retinal terminals that innervate proximal dendrites, and modulated by small cortical terminals that innervate distal dendrites (Jones and Powell 1969; Cleland et al. 1971; Hajdu

et al. 1982; Hamos et al. 1987; Vidnyanszky and Hamori 1994; Sherman and Guillery 1996, 1998; Sillito et al. 2006). The inputs from cortical layer V to the dorsal thalamus are similar to

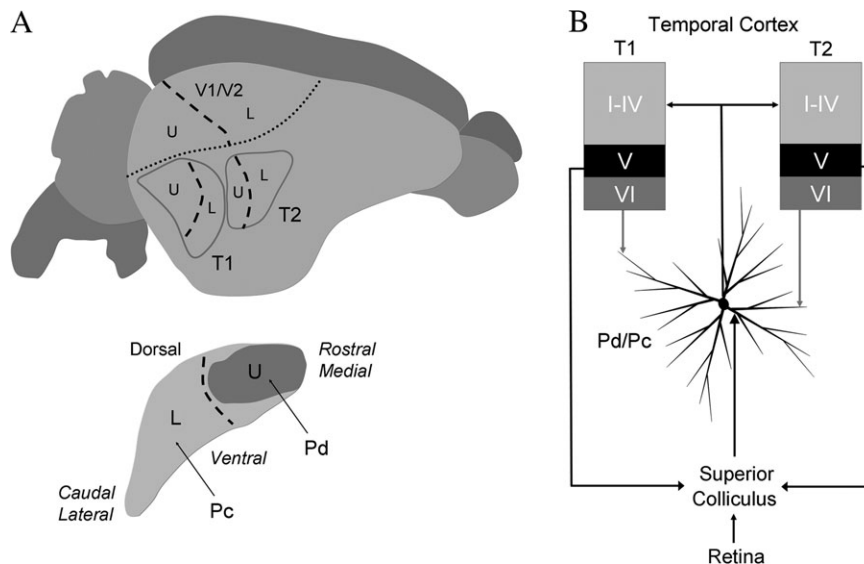


Figure 12. A summary of the results of the current study and those of our previous study of tectopulvinar projections (Chomsung et al. 2008). (A) A schematic depiction of the visual field representations (U, upper visual field, L, lower visual field, dashed line, horizontal meridian) within the pulvinar nucleus and temporal cortex estimated from the location of tectopulvinar cells and pulvinocortical terminals labeled following small injections of BDA in the pulvinar nucleus. (B) The Pd and Pc are reciprocally connected to 2 regions of the temporal cortex (T1 and T2). The Pd and Pc project to layers I-IV of T1 and T2 where they contact spines. In the Pd and Pc, projection cells receive input from the SC on proximal dendrites, and input from layer VI temporal cortex cells on distal dendrites. Because the SC receives input from the retina as well as layer V cells in the striate and temporal cortex, the Pd and Pc can be categorized as "second order" nuclei to indicate their unique position in integrating ascending input from the periphery with descending input from the cortex. V1, striate cortex, V2, secondary visual cortex.

retinogeniculate terminals. They are large terminals that participate in complex synaptic arrangements known as glomeruli, and contact proximal dendrites (Vidnyanszky et al. 1996; Erişir et al. 1997; Feig and Harting 1998; Li et al. 2003; Baldauf et al. 2005). Similarities in the excitatory postsynaptic potentials (EPSPs) elicited by stimulation of layer V corticothalamic terminals or retinogeniculate terminals *in vitro* have also been noted (Turner and Salt 1998; Chen et al. 2002; Li et al. 2003; Reichova and Sherman 2004). Thus, it has been suggested that layer V corticothalamic inputs drive thalamic responses in a manner similar to retinogeniculate inputs, and regions of the dorsal thalamus that receive input from cortical layer V are considered "higher order" nuclei because they may transfer layer V cortical information to other cortical areas (Guillery and Sherman 2002).

We found that the tectorecipient pulvinar nucleus cannot be classified as a higher order nucleus because we found that its cortical input arises exclusively from layer VI (confirming a previous report by Kawamura and Diamond 1978), and that corticopulvinar terminals in the Pd and Pc are all small terminals that primarily contact small caliber non-GABAergic dendrites. Furthermore, the Pd and Pc form reciprocal connections with the temporal cortex, whereas higher order nuclei form nonreciprocal connections (Van Horn and Sherman 2004; Llano and Sherman 2008).

On the other hand, several features of the tectorecipient pulvinar nucleus are different from those of first order nuclei. First the tectorecipient pulvinar does not contain the large glomerular terminals that are characteristic of the primary or driving inputs of first order nuclei (such as the retinal input to the dLGN; Hajdu et al. 1982). Although tectal terminals innervate proximal dendrites, they are smaller than retinogeniculate terminals and do not form glomeruli. Instead they form tubular clusters that surround central dendrites (Robson and Hall 1977; Kelly et al. 2003; Chomsung et al. 2008; Masterson

et al. 2009a), and preliminary studies have revealed that the characteristics of tectal EPSPs elicited *in vitro* are different from those of either corticothalamic EPSPs, or retinogeniculate EPSPs (Masterson et al. 2009b). Furthermore, the laminar distribution of pulvinocortical terminals originating from the Pd and Pc is different from that of geniculostriate terminals (Harting et al. 1973).

We therefore conclude that a third category is necessary to describe the organization of the tectorecipient pulvinar nucleus of the tree shrew. Traditionally, the retino-tectothalamocortical pathways have been considered secondary visual pathways that relay ascending sensory signals in parallel with the primary retino-geniculocortical pathways (Diamond and Hall 1969; Schneider 1969). Our anatomical results support the idea that the Pd and Pc are "second order" nuclei (Masterson et al. 2009a) that relay visual information from the SC to the temporal cortex, and that the activity of the Pd and Pc is modulated by the temporal cortex directly via layer VI corticothalamic projections, as well as indirectly via layer V corticotectal projections (Fig. 12B).

Relation to Primate Pulvinocortical Connections

The main tectorecipient zone of the primate pulvinar nucleus is the inferior subdivision. In the prosimian primate *Galago senegalensis* (lesser bushbaby), tectal terminals fill most of the inferior division of the pulvinar nucleus (Glendenning et al. 1975). In the new and old world simian primates, *Saimiri sciureus* (squirrel monkey), *Callithrix jacchus* (marmoset), and *Macaca mulatta* (macaque or rhesus monkey), tectal terminals are confined primarily to the posterior and central medial subdivisions of the inferior pulvinar (PIp and PIcm; Stepniewska et al. 2000).

In simian primates, retrograde tracing experiments have shown that the tectorecipient subdivisions PIp and PIcm

primarily project to cortical areas surrounding the middle temporal area (MT), which can be identified by dense myelin staining (Cusick et al. 1993; Stepniewska et al. 1999, 2000; Kaas and Lyon 2007). Furthermore, pulvinar neurons which can be orthodromically activated from the SC are intermingled with cells that can be antidromically activated from area MT (Berman and Wurtz 2008). Based on its extensive connections with V1, it has been suggested that the tree shrew area Td is a possible homolog of the primate area MT (Sesma et al. 1984; Lyon et al. 1998). However, the myelin pattern used to identify area MT in primates is much less apparent in tree shrews (Wong and Kaas 2009).

Anterograde tracing studies of the cortical projections of the tectorecipient pulvinar of simian primates have not yet been carried out. However, anterograde degeneration studies of the *Galago* indicate that the projections from the tectorecipient subdivision of the pulvinar nucleus are very similar to those that we have identified in the current study. Lesions confined to the inferior pulvinar nucleus resulted in the degeneration of terminals in the temporal cortex, and many of the lesions resulted in 2 patches of degeneration, with one patch overlapping area MT, and another in the ventral temporal cortex (Glendenning et al. 1975). Although it was concluded that MT is the primary target of the *Galago* tectorecipient pulvinar, the pattern of pulvinocortical projections is strikingly similar to our observations in the tree shrew.

Behavioral studies of *Galago* indicate that lesions of area MT impair the ability of animals to locate an object in space (Wilson et al. 1979), whereas lesions of the ventral temporal cortex impair the ability of animals to learn visual discrimination tasks (Diamond and Hall 1969; Killackey et al. 1971; Atencio et al. 1975). A role for pulvinocortical pathways in pattern discrimination was further demonstrated by the finding that lesions of the inferior (but not the lateral or medial) pulvinar nucleus of macaque monkeys impaired visual pattern discrimination learning (Chalupa et al. 1976). Behavioral studies of tree shrews further indicate that tecto-pulvinocortical pathways play a major role in pattern discrimination because this ability is impaired after lesions confined to the superficial layers of the SC (where tectopulvinar cells are located), or after lesions of the ventral temporal cortex (Casagrande and Diamond 1974).

However, despite the many similarities in the organization of tecto-pulvino-cortical pathways of tree shrews and primates, the tree shrew is distinguished from primates by the relative lack of visual impairment after ablation of the entire striate cortex. Although *Galagos* and other primates exhibit a profound sensory loss after ablation of V1, deficits in tree shrews are only revealed when the animals attempt to discriminate very complex images (Diamond and Hall 1969; Killackey et al. 1971; Ware et al. 1974; Atencio et al. 1975). It has been proposed that the expanded tectopulvinar pathway of the tree shrew underlies this difference. In fact, it has been estimated that the tree shrew SGS has a volume that is approximately one-half the size of its striate cortex, and 6 times greater than its dLGN. In comparison, the macaque SGS is about one-fifth the volume of its dLGN (Norton 1982).

Another difference between the tree shrew and primate is that the tectorecipient and striate-recipient zones of the pulvinar nucleus are clearly segregated in the tree shrew, but show a considerable degree of overlap in primates. In tree

shrews, projections from the striate cortex to the extrageniculate thalamus are limited to the ventral pulvinar nucleus and lateral intermediate nucleus (Huerta et al. 1985; Day-Brown et al. 2007), and, as demonstrated in the current study, only the temporal cortex projects to the Pd and Pc. In contrast, the tectorecipient zones of the primate pulvinar nucleus receive extensive input from both the striate and temporal cortex (Glendenning et al. 1975; Symonds and Kaas 1978; Lin and Kaas 1979; Raczkowski and Diamond 1980, 1981; Wall et al. 1982; Ungerleider et al. 1983). Furthermore, the majority of the striate cortex input to the primate pulvinar nucleus is in the form of large glomerular terminals characteristic of higher order nuclei (Ogren and Hendrickson 1979).

This difference in the organization of the tectorecipient zones of the primate pulvinar nucleus and that of other species could account for the conflicting accounts regarding the effects of SC input on pulvinar response properties. In the macaque, lesions of the SC have little effect on the response properties of neurons in the tectorecipient zone of the pulvinar nucleus, whereas lesions of the striate cortex greatly diminished their visual responsiveness (Bender 1983). In contrast, lidocaine injections in the SC of the rabbit greatly reduce the responsiveness of neurons in the lateral posterior nucleus, and this effect is topographic (Casanova and Molotchnikoff 1990).

An increased dependence on input from the striate cortex may distinguish the tectorecipient regions of the primate pulvinar nucleus from that of the tree shrew, and this organization may be reflected in the more severe sensory deficits following striate cortex damage. Thus, although studies of the tree shrew suggest that tectopulvinar-cortical pathways play a role in pattern vision, it remains unclear whether this is the case in primates. The current study provides further evidence that the tree shrew offers a model system to investigate the tectopulvinar and striate-pulvinar pathways in relative isolation to help clarify their respective roles in vision.

Conclusions

The main contribution of this study is the characterization of the synaptic organization of pulvinocortical projections. Projections from the tectorecipient zones of the pulvinar nucleus are densely distributed in the temporal cortex, forming 2 topographic maps. In contrast to the horizontal arrangement of geniculocortical terminals, pulvinocortical terminals are arranged in columns; the spines postsynaptic to pulvinocortical terminals likely arise from the apical dendrites of pyramidal cells.

In addition, we have more clearly defined the unique circuitry of the tectorecipient zones of the tree shrew pulvinar nucleus. Although other regions of the pulvinar nucleus can be categorized as higher order based on their direct innervation by cortical layer V, the only direct cortical inputs to the Pd and Pc originate from layer VI cells which form small terminals that innervate small caliber dendrites. Furthermore, all connections with the temporal cortex appear to be reciprocal. Thus, it does not appear that the Pd and Pc receive input from one cortical area and transfer this information to other cortical areas (the proposed function of higher order nuclei, Guillery 1995; Guillery and Sherman 2002). Instead, we hypothesize that the SC drives the responses of Pd and Pc cells, which may subsequently influence behavior by activating subcortical visuomotor circuits.

Funding

National Institutes of Health grant number (NS35377 and EY016155); and Grant sponsor Sigma Xi.

Notes

The authors thank Dr William C. Hall for his helpful comments on the manuscript, Mr Michael A. Eisenback, Mr Arkadiusz S. Slusarczyk, and Ms Cathie G. Caple for their expert technical assistance with the confocal and electron microscopy, and the University of Louisville Research Resources Center for their assistance with animal surgeries and maintenance of the tree shrew colony. *Conflict of Interest:* None declared.

Address correspondence to Martha E. Bickford, PhD, Department of Anatomical Sciences and Neurobiology, University of Louisville, School of Medicine, 500 S. Preston St., Louisville, KY 40292, USA. Email: martha.bickford@louisville.edu.

References

- Anderson JC, Maçarico da Costa N, Martin KA. 2009. The W cell pathway to cat primary visual cortex. *J Comp Neurol*. Article Accepted Online: Apr 3 2009.
- Atencio FW, Diamond IT, Ward JP. 1975. Behavioral study of the visual cortex of *Galago senegalensis*. *J Comp Physiol Psychol*. 89(10):1109-1135.
- Baldauf ZB, Chomsung RD, Carden WB, May PJ, Bickford ME. 2005. Ultrastructural analysis of projections to the pulvinar nucleus of the cat. I: middle suprasylvian gyrus (areas 5 and 7). *J Comp Neurol*. 485:87-107.
- Bender DB. 1983. Visual activation of neurons in the primate pulvinar depends on cortex but not colliculus. *Brain Res*. 279(1-2):258-261.
- Berman RA, Wurtz RH. 2008. Exploring the pulvinar path to visual cortex. *Prog Brain Res*. 2008;171:467-473.
- Campbell CBG. 1980. The nervous system of tupaiidae: its bearing on phyletic relationships. In: Luckett WP, editor. *Comparative biology and evolutionary relationships of tree shrews*. New York: Plenum Press. p. 219-242.
- Casagrande VA, Diamond IT. 1974. Ablation study of the superior colliculus in the tree shrew (*Tupaia glis*). *J Comp Neurol*. 156:207-238.
- Casanova C, Molotchnikoff S. 1990. Influence of the superior colliculus on visual responses of cells in the rabbit's lateral posterior nucleus. *Exp Brain Res*. 80(2):387-396.
- Chalupa KM, Coyle RS, Lindsley DB. 1976. Effect of pulvinar lesions on visual pattern discrimination in monkeys. *J Neurophysiol*. 39(2):354-369.
- Chen C, Blitz DM, Regehr WG. 2002. Contributions of receptor desensitization and saturation to plasticity at the retinogeniculate synapse. *Neuron*. 33:779-788.
- Chomsung RD, Petry HM, Bickford ME. 2008. Ultrastructural examination of diffuse and specific tectopulvinar projections in the tree shrew. *J Comp Neurol*. 510:24-46.
- Cleland BG, Dubin MW, Levick WR. 1971. Sustained and transient neurones in the cat's retina and lateral geniculate nucleus. *J Physiol*. 217(2):473-496.
- Cowey A. 2009. The blindsight saga. *Exp Brain Res*. Epub ahead of print.
- Cusick CG, Scriptor JL, Darenbourg JG, Weber JT. 1993. Chemoarchitectonic subdivisions of the visual pulvinar in monkeys and their connective relations with the middle temporal and rostral dorsolateral visual areas, MT and DLr. *J Comp Neurol*. 336:1-30.
- Cusick CG, Steindler DA, Kaas JH. 1985. Corticocortical and collateral thalamocortical connections of postcentral somatosensory cortical areas in squirrel monkeys: a double-labeling study with radiolabeled wheatgerm agglutinin and wheatgerm agglutinin conjugated to horseradish peroxidase. *Somatosens Res*. 3(1):1-31.
- Day-Brown JD, Chomsung RD, Petry HM, Bickford ME. 2007. Synaptic organization of striate cortex projections to the tree shrew dorsal thalamus. *Soc Neurosci Abstr*. 392.7:112.
- Diamond IT, Hall WC. 1969. Evolution of neocortex. *Science*. 164:251-262.
- Diamond IT, Snyder M, Killackey H, Jane J, Hall WC. 1970. Thalamocortical projections in the tree shrew (*Tupaia glis*). *J Comp Neurol*. 139:273-306.
- Ding Y, Casagrande VA. 1998. Synaptic and neurochemical characterization of parallel pathways to the cytochrome oxidase blobs of primate visual cortex. *J Comp Neurol*. 391:429-443.
- Einstein G, Davis TL, Sterling P. 1987. Ultrastructure of synapses from the A-laminae of the lateral geniculate nucleus in layer IV of the cat striate cortex. *J Comp Neurol*. 260:63-75.
- Erisir A, Dreusicke M. 2005. Quantitative morphology and postsynaptic targets of thalamocortical axons in critical period and adult ferret visual cortex. *J Comp Neurol*. 485:11-31.
- Erişir A, Van Horn SC, Sherman SM. 1997. Relative numbers of cortical and brainstem inputs to the lateral geniculate nucleus. *Proc Natl Acad Sci U S A*. 94(4):1517-1520.
- Feig S, Harting JK. 1998. Cortico-cortical communication via the thalamus: Ultrastructural studies of corticothalamic projections from area 17 to the lateral posterior nucleus of the cat and inferior pulvinar nucleus of the owl monkey. *J Comp Neurol*. 395(3):281-295.
- Geneser-Jensen FA, Blackstad JW. 1971. Distribution of acetylcholinesterase in the hippocampal region of the guinea pig. I. Entorhinal area, subiculum and presubiculum. *Z Zellforsch Mikrosk Anat*. 114:460-481.
- Glendenning KK, Hall JA, Diamond IT, Hall WC. 1975. The pulvinar nucleus of the *Galago senegalensis*. *J Comp Neurol*. 16:419-458.
- Guillery RS. 1995. Anatomical evidence concerning the role of the thalamus in corticocortical communication: a brief review. *J Anat*. 187(Pt 3):583-592.
- Guillery RW, Sherman SM. 2002. Thalamic relay functions and their role in corticocortical communication: generalizations from the visual system. *Neuron*. 33(2):163-175.
- Hajdu F, Hassler R, Somogyi G. 1982. Neuronal and synaptic organization of the lateral geniculate nucleus of the tree shrew, *Tupaia glis*. *Cell Tissue Res*. 224(1):207-223.
- Hamos JE, Van Horn SC, Raczkowski D, Sherman SM. 1987. Synaptic circuits involving an individual retinogeniculate axon in the cat. *J Comp Neurol*. 259(2):165-192. Erratum in: *J Comp Neurol*. 260(3):481.
- Harting JK, Diamond IT, Hall WC. 1973. Anterograde degeneration study of the cortical projections of the lateral geniculate and pulvinar nuclei in the tree shrew (*Tupaia glis*). *J Comp Neurol*. 150:393-440.
- Huerta MF, Wber JT, Rothstein LR, Harting JK. 1985. Subcortical connections of area 17 in the tree shrew: an autoradiographic analysis. *Brain Res*. 340(1):163-170.
- Huppé-Gourgues F, Bickford ME, Boire D, Pito M, Casanova C. 2006. Distribution, morphology, and synaptic targets of corticothalamic terminals in the cat lateral posterior-pulvinar complex that originate from the posteromedial lateral suprasylvian cortex. *J Comp Neurol*. 497(6):847-863.
- Jones EG, Powell TP. 1969. An electron microscopic study of the mode of termination of cortico-thalamic fibres within the sensory relay nuclei of the thalamus. *Proc R Soc Lond B Biol Sci*. 172:173-185.
- Kaas JH. 2002. Convergences in the modular and areal organization of the forebrain of mammals: implications for the reconstruction of forebrain evolution. *Brain Behav Evol*. 59:262-272.
- Kaas JH, Lyon DC. 2007. Pulvinar contributions to the dorsal and ventral streams of visual processing in primates. *Brain Res Rev*. 55(2):285-296.
- Kaas JH, Preuss TM. 1993. Archontan affinities as reflected in the visual system. In: Szalay R, Novacek M, Mckenna M, editors. *Mammal phylogeny: placentals*. New York: Springer-Verlag. p. 115-128.
- Kaufman EF, Rosenquist AC, Raczkowski D. 1984. The projections of single thalamic neurons onto multiple visual cortical areas in the cat. *Brain Res*. 298(1):171-174.
- Kawamura S, Diamond IT. 1978. The laminar origin of descending projections from the cortex to the thalamus in *Tupaia glis*. *Brain Res*. 153:333-339.

- Kelly LR, Li J, Carden WB, Bickford ME. 2003. Ultrastructure and synaptic targets of tectothalamic terminals in the cat lateral posterior nucleus. *J Comp Neurol*. 464:472-486.
- Killackey H, Snyder M, Diamond IT. 1971. Function of striate and temporal cortex in the tree shrew. *J Comp Physiol Psychol*. 74:1-29.
- Lane RH, Allman JM, Kaas JH. 1971. Representation of the visual field in the superior colliculus of the grey squirrel (*Sciurus carolinensis*) and the tree shrew (*Tupaia glis*). *Brain Res*. 26:277-292.
- Latawiec D, Martin KA, Meskenaite V. 2000. Termination of the geniculocortical projection in the striate cortex of macaque monkey: a quantitative immunoelectron microscopic study. *J Comp Neurol*. 419:306-319.
- LeGros Clark WE. 1934. Early forerunners of man. London: Baillere, Tynndall and Cox.
- Li J, Wang S, Bickford ME. 2003. Comparison of the ultrastructure of cortical and retinal terminals in the rat dorsal lateral geniculate and lateral posterior nuclei. *J Comp Neurol*. 460:394-409.
- Lin CS, Kaas JH. 1979. The inferior pulvinar complex in owl monkeys: architectonic subdivisions and patterns of input from the superior colliculus and subdivisions of visual cortex. *J Comp Neurol*. 187(4):655-678.
- Llano DA, Sherman SM. 2008. Evidence for nonreciprocal organization of the mouse auditory thalamocortical-corticothalamic projection systems. *J Comp Neurol*. 507(2):1209-1227.
- Luppino G, Matelli M, Carey RG, Fitzpatrick D, Diamond IT. 1988. New view of the organization of the pulvinar nucleus in Tupaia as revealed by tectopulvinar and pulvinar-cortical projections. *J Comp Neurol*. 273:67-86.
- Lyon DC, Jain N, Kaas JH. 1998. Cortical connections of striate and extrastriate visual areas in tree shrews. *J Comp Neurol*. 401:109-128.
- Lyon DC, Jain N, Kaas JH. 2003a. The visual pulvinar in tree shrews I. Multiple subdivisions revealed through acetylcholinesterase and Cat-301 chemoarchitecture. *J Comp Neurol*. 467:593-606.
- Lyon DC, Jain N, Kaas JH. 2003b. The visual pulvinar in tree shrews II. Projections of four nuclei to areas of visual cortex. *J Comp Neurol*. 467:607-627.
- Masterson SP, Li J, Bickford ME. 2009a. Synaptic organization of the tectorecipient zone of the rat lateral posterior nucleus. *J Comp Neurol*. 515:24-46.
- Masterson SP, Li J, Bickford ME. 2009b. Substance P-mediated long term potentiation in the visual thalamus. *Soc Neurosci Abstr*. 35:319.
- Miceli D, Reperant J, Marchand L, Ward R, Vesselkin N. 1991. Divergence and collateral axon branching in subsystems of visual cortical projections from the cat lateral posterior nucleus. *J Hirnforsch*. 32(2):165-173.
- Muly EC, Fitzpatrick D. 1992. The morphological basis for binocular and ON/OFF convergence in tree shrew striate cortex. *J Neurosci*. 12(4):1319-1334.
- Nahmani M, Erisir A. 2005. VGluT2 immunocytochemistry identifies thalamocortical terminals in layer 4 of adult and developing visual cortex. *J Comp Neurol*. 484:458-473.
- Norton TT. 1982. Geniculate and extrageniculate visual systems in the tree shrew. In: Changing concepts of the nervous system. New York: Academic Press, Inc. p. 377-409.
- Ogren MP, Hendrickson AE. 1979. The morphology and distribution of striate cortex terminals in the inferior and lateral subdivisions of the Macaca monkey pulvinar. *J Comp Neurol*. 188(1):179-199.
- Patel NC, Bickford ME. 1997. Synaptic targets of cholinergic terminals in the pulvinar nucleus of the cat. *J Comp Neurol*. 387(2):266-278.
- Raczkowski D, Diamond IT. 1980. Cortical connections of the pulvinar nucleus in Galago. *J Comp Neurol*. 193(1):1-40.
- Raczkowski D, Diamond IT. 1981. Projections from the superior colliculus and the neocortex to the pulvinar nucleus in Galago. *J Comp Neurol*. 200(2):231-254.
- Raczkowski D, Fitzpatrick D. 1990. Terminal arbors of individual, physiologically identified geniculocortical axons in the tree shrew's striate cortex. *J Comp Neurol*. 302(3):500-514.
- Reichova I, Sherman SM. 2004. Somatosensory corticothalamic projections: distinguishing drivers from modulators. *J Neurophysiol*. 92(4):2185-2197.
- Robson JA, Hall WC. 1977. The organization of the pulvinar in the grey squirrel (*Sciurus carolinensis*). II. Synaptic organization and comparisons with the dorsal lateral geniculate nucleus. *J Comp Neurol*. 173:389-416.
- Rockland KS, Andersen J, Cowie RJ, Robinson DL. 1999. Single axon analysis of pulvinocortical connections to several visual areas in the macaque. *J Comp Neurol*. 406(2):221-250.
- Schneider GE. 1969. Two visual systems. *Science*. 163:895-902.
- Sesma MA, Casagrande VA, Kaas JH. 1984. Cortical connections of area 17 in tree shrews. *J Comp Neurol*. 230:337-351.
- Sherman MS, Guillery RW. 1996. Functional Organization of thalamocortical relays. *J Neurosci*. 16:1367-1395.
- Sherman MS, Guillery RW. 1998. On the actions that one nerve cell can have on another: distinguishing "drivers" from "modulators". *Proc Natl Acad Sci USA*. 95:7121-7126.
- Sillito AM, Cudeiro J, Jones HE. 2006. Always returning: feedback and sensory processing in visual cortex and thalamus. *Trends Neurosci*. 29:307-316.
- Smith PH, Populin LC. 2001. Fundamental differences between the thalamocortical recipient layers of the cat auditory and visual cortices. *J Comp Neurol*. 436:508-519.
- Stepniewska I, Qi HX, Kaas JH. 1999. Do superior colliculus projection zones in the inferior pulvinar project to MT in primates? *Eur J Neurosci*. 11:469-480.
- Stepniewska I, Qi HX, Kaas JH. 2000. Projections of the superior colliculus to subdivisions of the inferior pulvinar in New World and Old World monkeys. *Vis Neurosci*. 17:529-549.
- Symonds LL, Kaas JH. 1978. Connections of striate cortex in prosimian, *Galago senegalensis*. *J Comp Neurol*. 181:477-512.
- Tong L, Spear PD. 1986. Single thalamic neurons project to both lateral suprasylvian visual cortex and area 17: a retrograde fluorescent double-labeling study. *J Comp Neurol*. 246(2):254-264.
- Turner JP, Salt TE. 1998. Characterization of sensory and corticothalamic excitatory inputs to rat thalamocortical neurones in vitro. *J Physiol*. 510:829-843.
- Ungerleider LG, Galkin TW, Mishkin M. 1983. Visuotopic organization of projections from striate cortex to inferior and lateral pulvinar in rhesus monkey. *J Comp Neurol*. 217:137-157.
- Van Horn SC, Sherman SM. 2004. Differences in projection patterns between large and small corticothalamic terminals. *J Comp Neurol*. 475:406-415.
- Vidnyanszky Z, Borostyankoi Z, Gorcs TJ, Hamori J. 1996. Light and electron microscopic analysis of synaptic input from cortical area 17 to the lateral posterior nucleus in cats. *Exp Brain Res*. 109:63-70.
- Vidnyanszky Z, Hamori J. 1994. Quantitative electron microscopic analysis of synaptic input from cortical areas 17 and 18 to the dorsal lateral geniculate nucleus in cats. *J Comp Neurol*. 349:259-268.
- Wall JT, Symonds LL, Kaas JH. 1982. Cortical and subcortical projections of the middle temporal area (MT) and adjacent cortex in galagos. *J Comp Neurol*. 211(2):193-214.
- Ware CB, Diamond IT, Casagrande VA. 1974. Effects of ablating the striate cortex on a successive pattern discrimination: further study of the visual system in the tree shrew (*Tupaia glis*). *Brain Behav Evol*. 9(4):264-279.
- Wilson M, Keys W, Johnston TD. 1979. Middle temporal cortical visual area and visuospatial function in Galago senegalensis. *J Comp Physiol Psychol*. 93(2):247-259.
- Wong P, Kaas JH. 2009. Architectonic subdivisions of neocortex in the tree shrew (*Tupaia belangeri*). *Anat Rec*. 292:994-1027.